Characteristics of Atmospheric-pressure Microgap Glow discharge Excited by Microwave Aiming at VUV Light Source

A. Kono T. Shibata and M. Aramaki

Department of Electrical Engineering and Computer Science
Nagoya University

Outline

- **Microwave-excited microgap discharge:**
  ***cw*, high-pressure, high-density, non-thermal plasma**

- **Electron temperature and density measurements by laser Thomson scattering**

- **Gas temperature characteristics**
    - **OES measurements**
    - **Fluid dynamic simulation for heat transport**

- **Preliminary VUV emission measurements**

- **Summary**

A comparison

Discharge pumped excimer laser | **Discharge in a microgap**

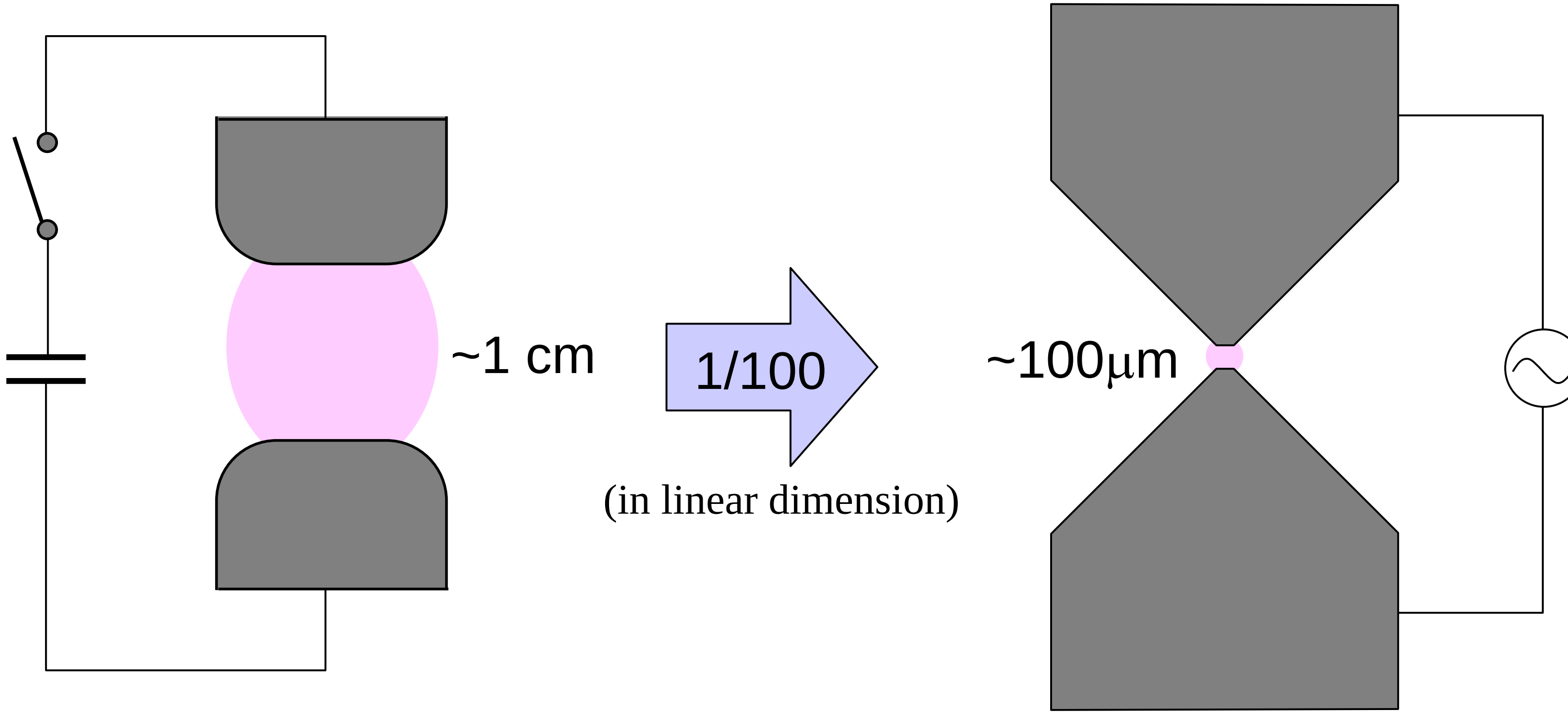

Pulsed
$\Delta t \sim$ 100ns

$p \sim 1$ atm
$n_e \sim 10^{15}$ cm^{-3}
$\varepsilon \sim 1$ MW cm^{-3}
$T_g \ll T_e$

→ ***CW*** plasma production with similar parameters?

Concept of high-pressure microgap discharge

- **Non-equilibrium plasma**

$$\frac{(d/\pi)^2}{D} < \frac{1}{n_e \sigma_m v_e} \cdot \frac{M}{m_e}$$

Diffusion lifetime Heating time

$$n_e = 10^{15}\ \mathrm{cm}^3 \longrightarrow d \sim 100\ \mu\mathrm{m}$$

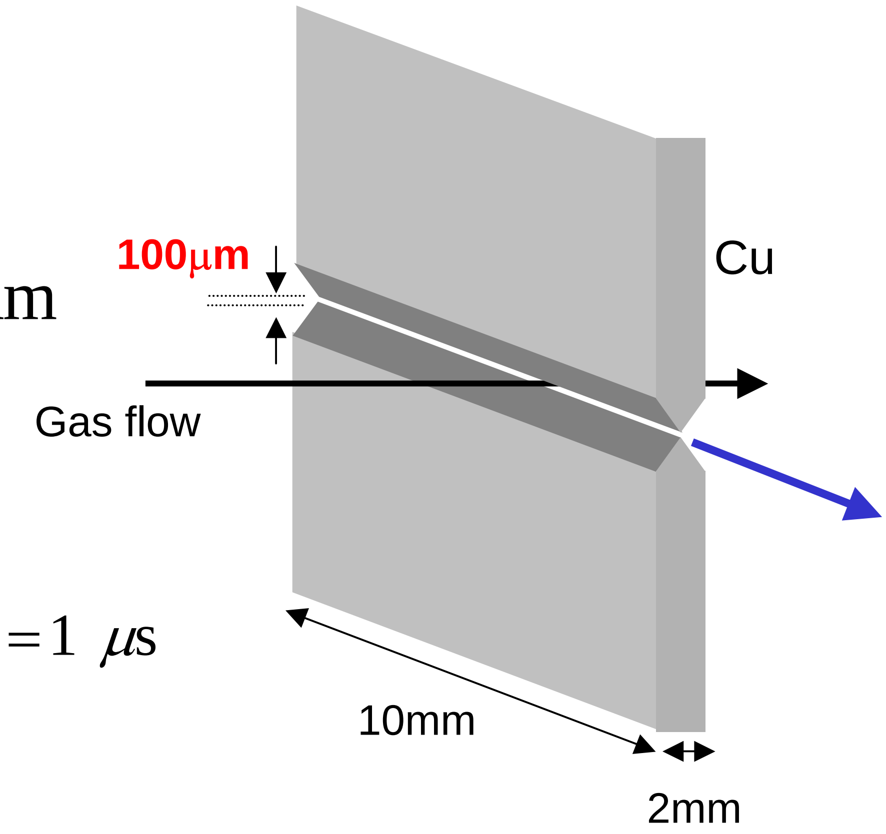

- **Rapid gas replacement**

$$\tau = \frac{w}{v_{flow}} \quad v_{flow} = 100\ \mathrm{m/s} \quad d = 100\ \mu\mathrm{m} \longrightarrow \tau = 1\ \mu s$$

- **Stable discharge**
- **High power-density deposition**

DC or RF excitation leads to discharge constriction

DC

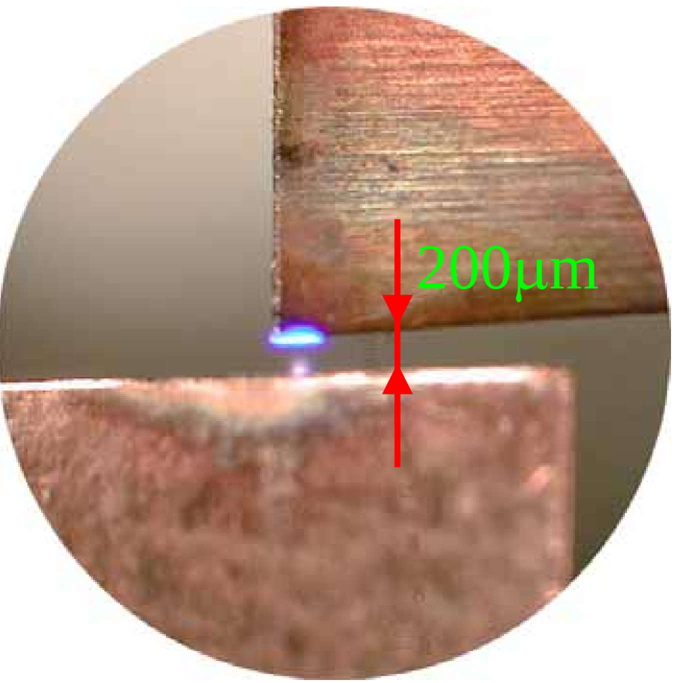

DC or RF(13.56MHz)

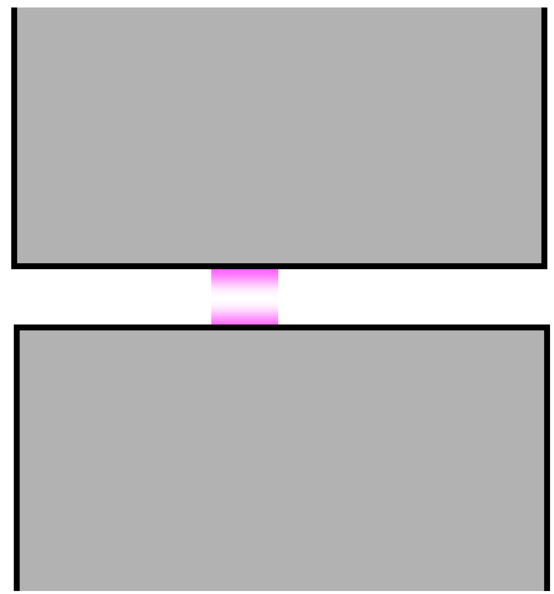

Microwave

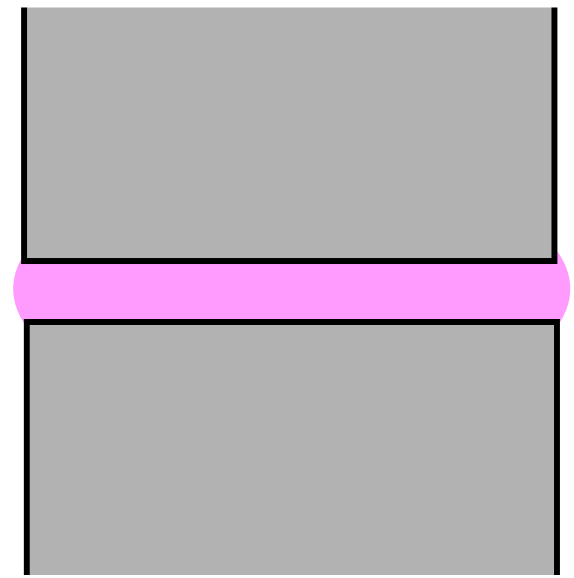

Microwave power transfer to the microgap

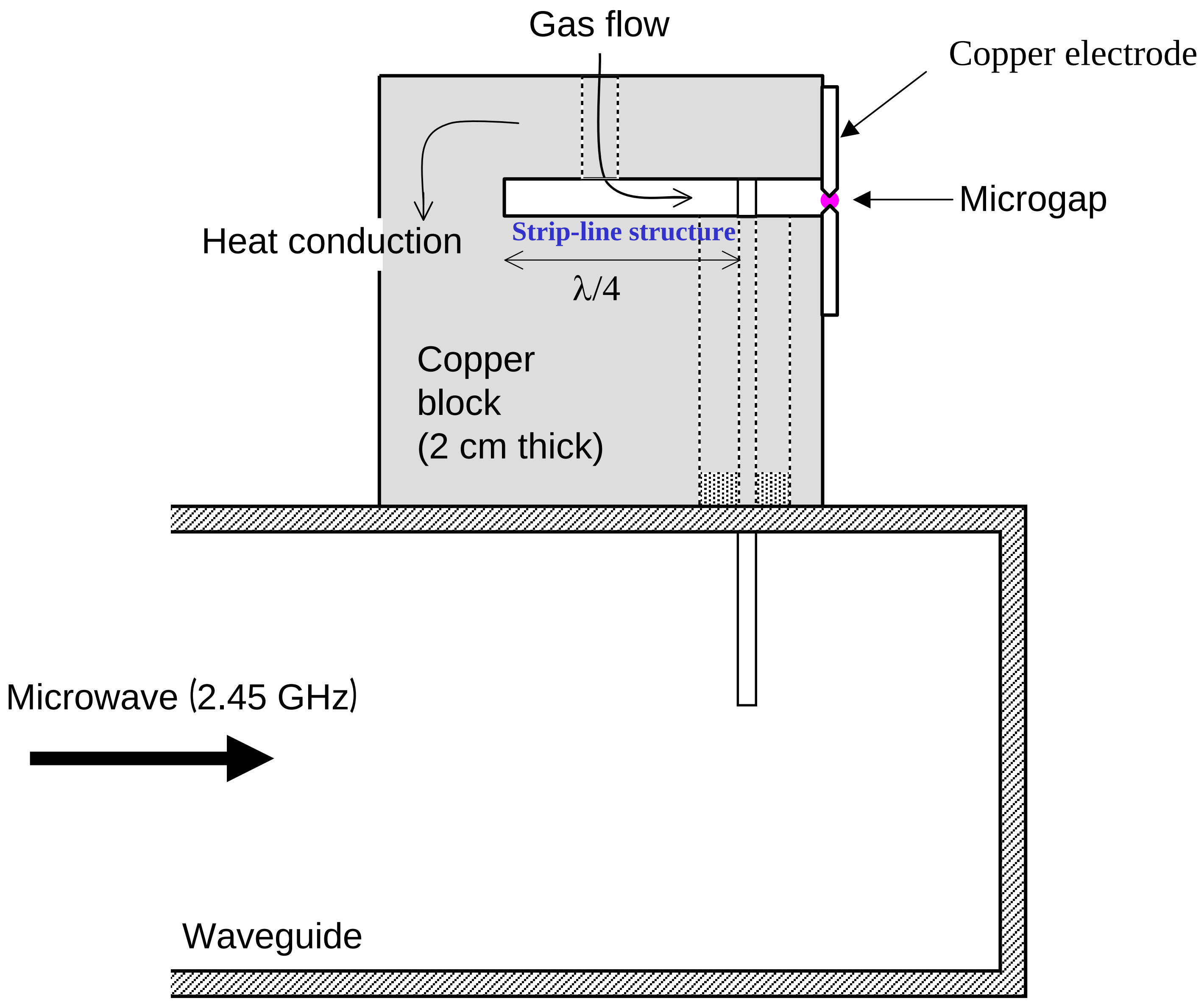

Microgap discharge in air (100 W)

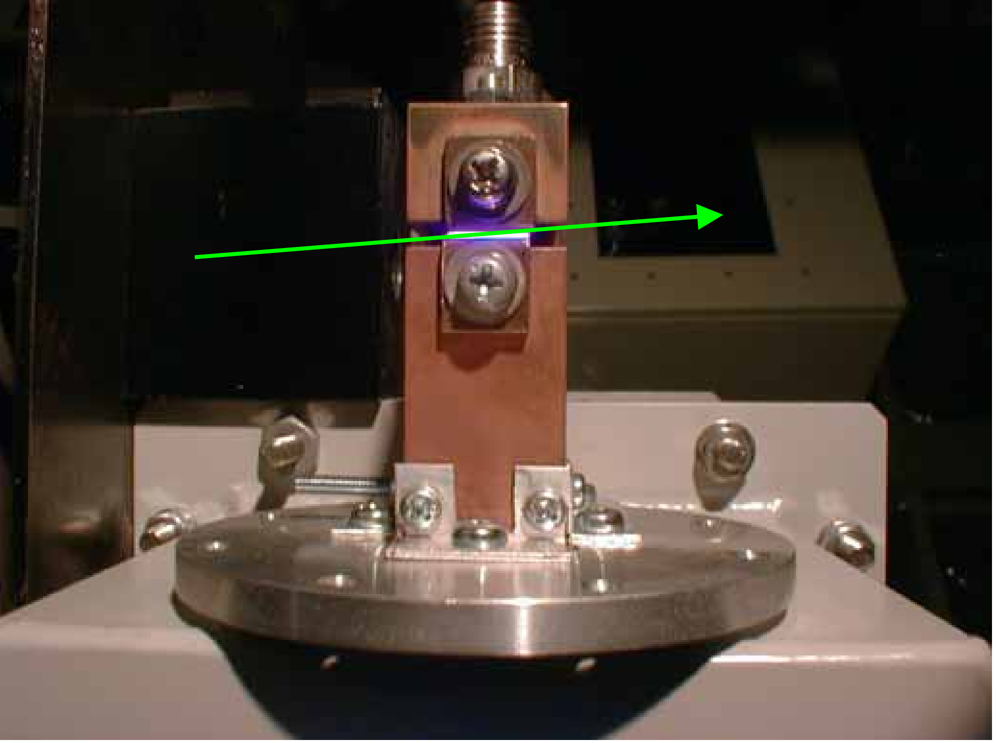

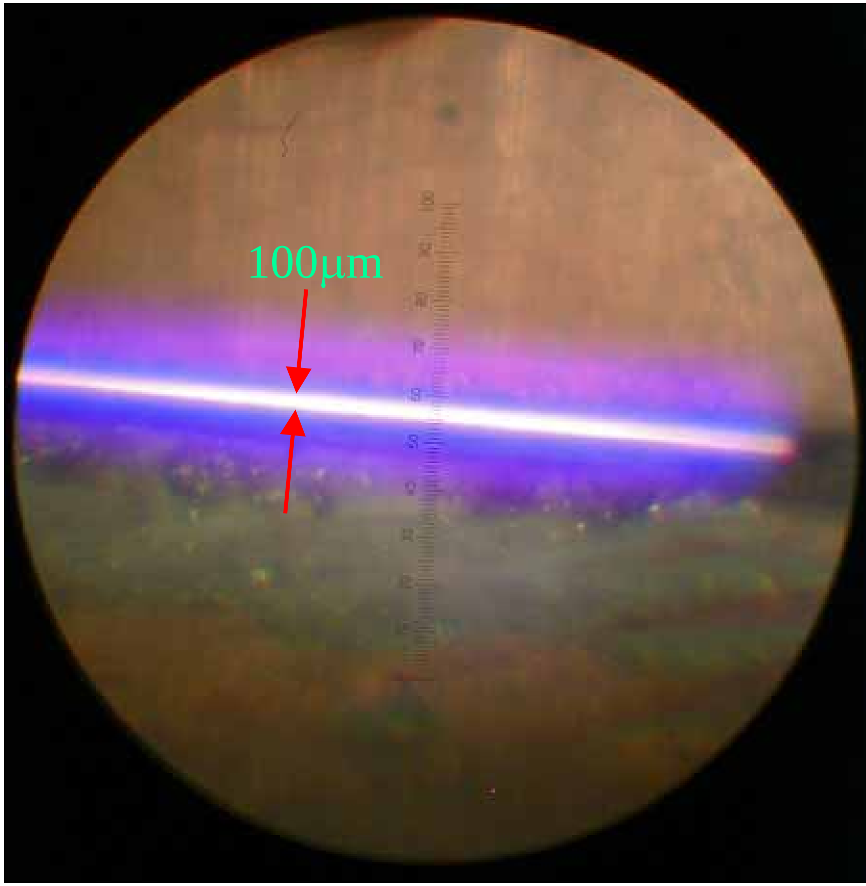

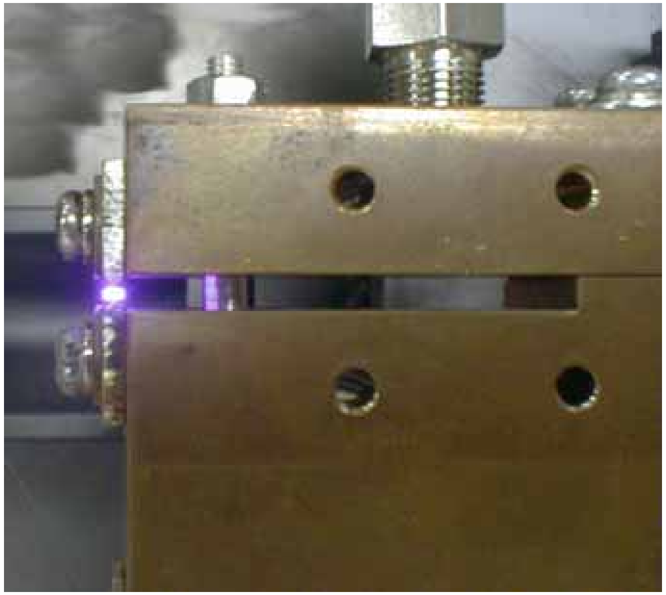

High-spatial-resolution Thomson scattering measurement

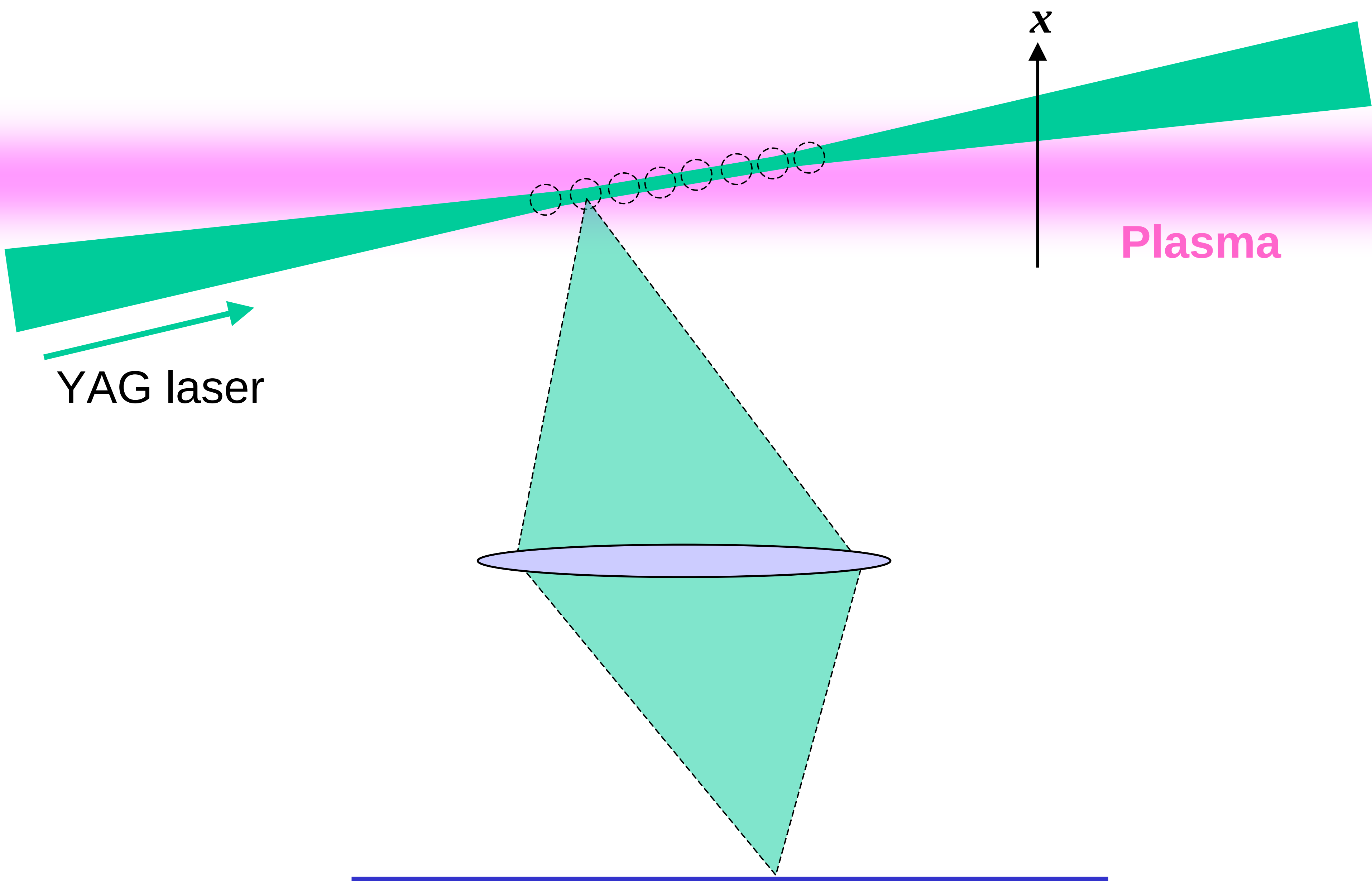

High-spatial-resolution Thomson scattering measurement

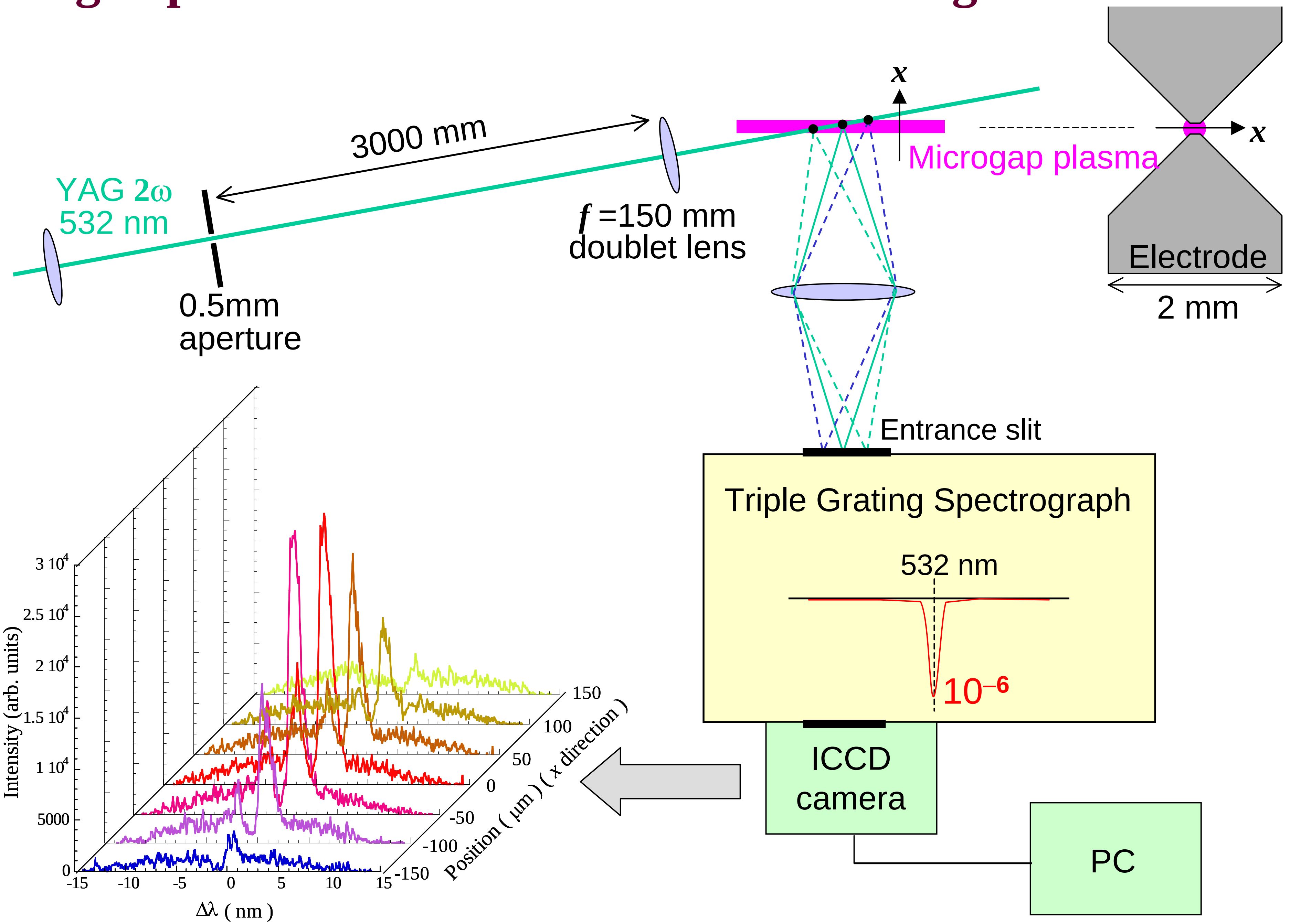

Fitting of the observed Thomson/Raman spectra

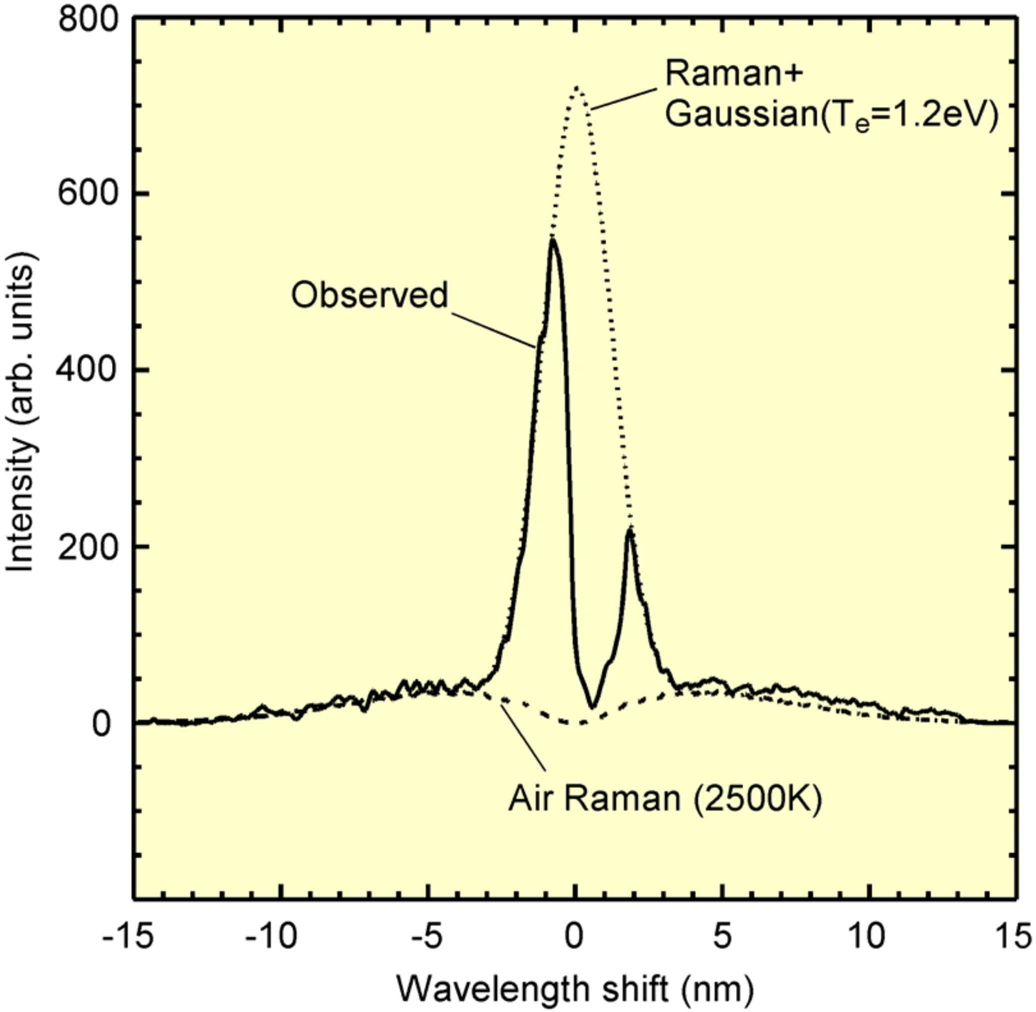

air 1atm ,
no gas flow,
microwave power 100W

Spatial distribution of n_e and T_e for air discharge

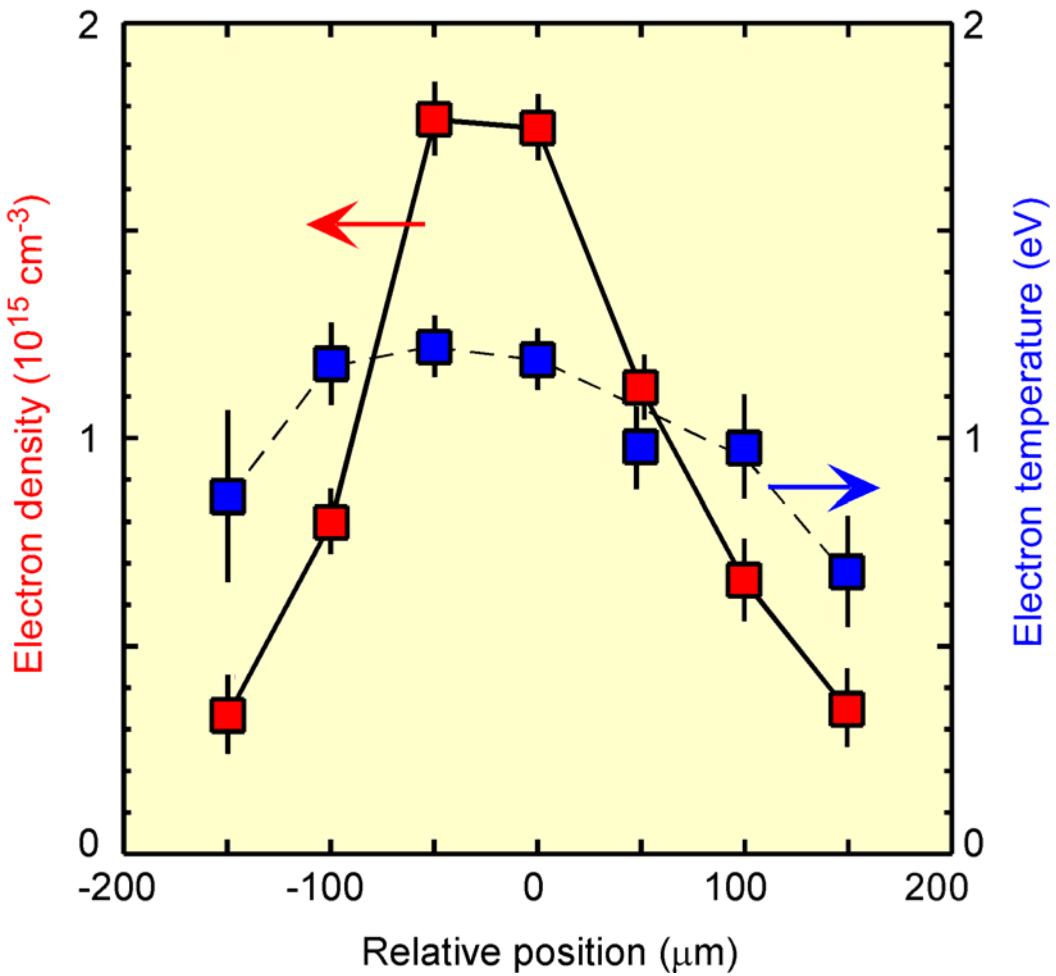

air 1atm ,
no gas flow,
microwave power 100W

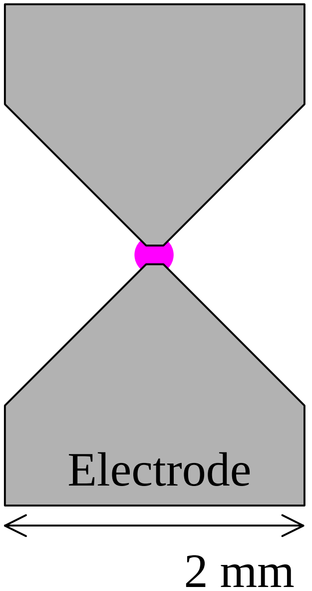

Comparison between air and He/N_2(5%) discharges

Thomson spectra at the plasma center

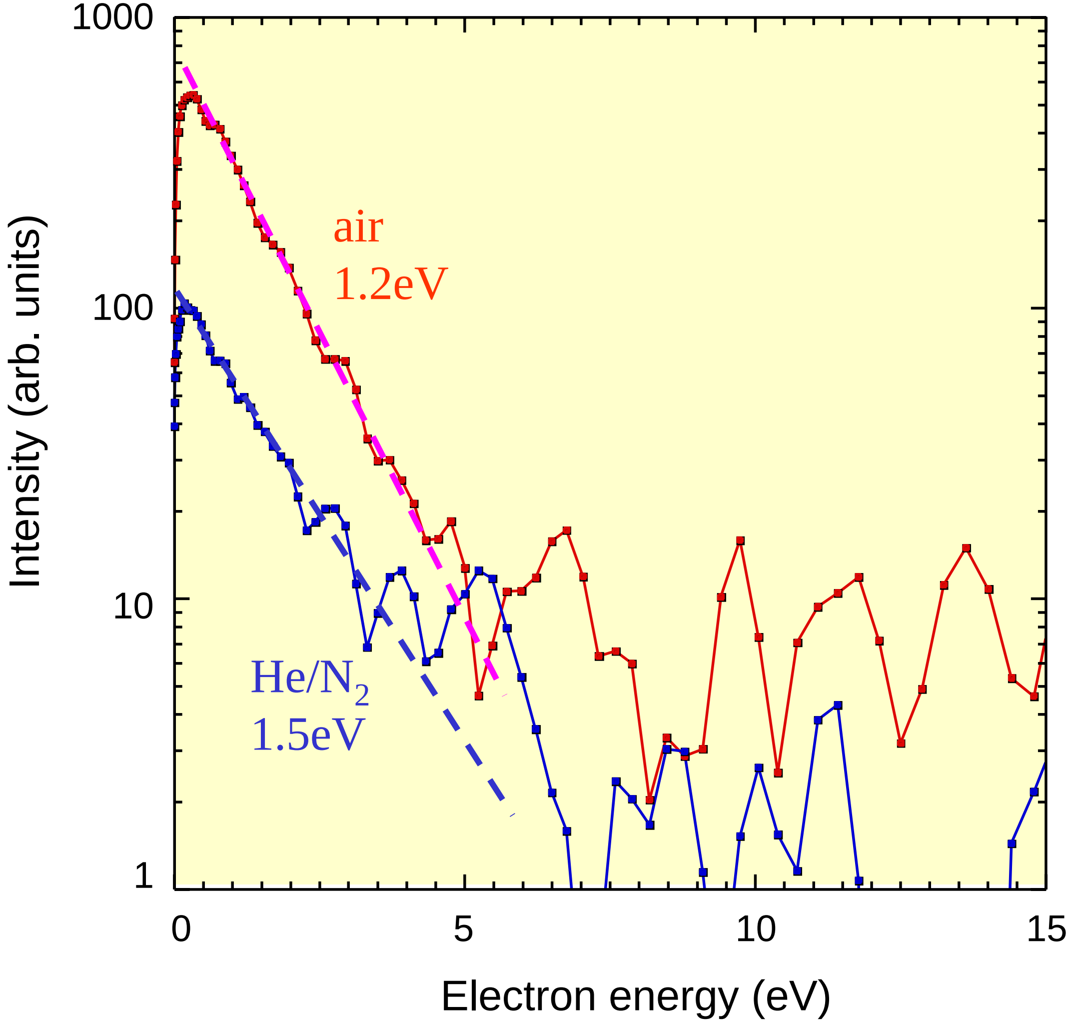

Discharge without chamber (1 atm)
μwave power 100W

***T_g*~2500K** for air
***T_g*~1200K** for He/N_2
(from Raman)

Electron density and temperature for different plasmas

Working gas	Air	He/N_2(5%)	Ar
Conditions	100 W No flow	100 W Slow flow	8 W 2 L/min
n_e (cm^{-3})	1.8×10^{15}	3×10^{14}	3×10^{14}
T_e (eV)	1.2	1.5	1.2

Preliminary VUV emission measurements

Spectra

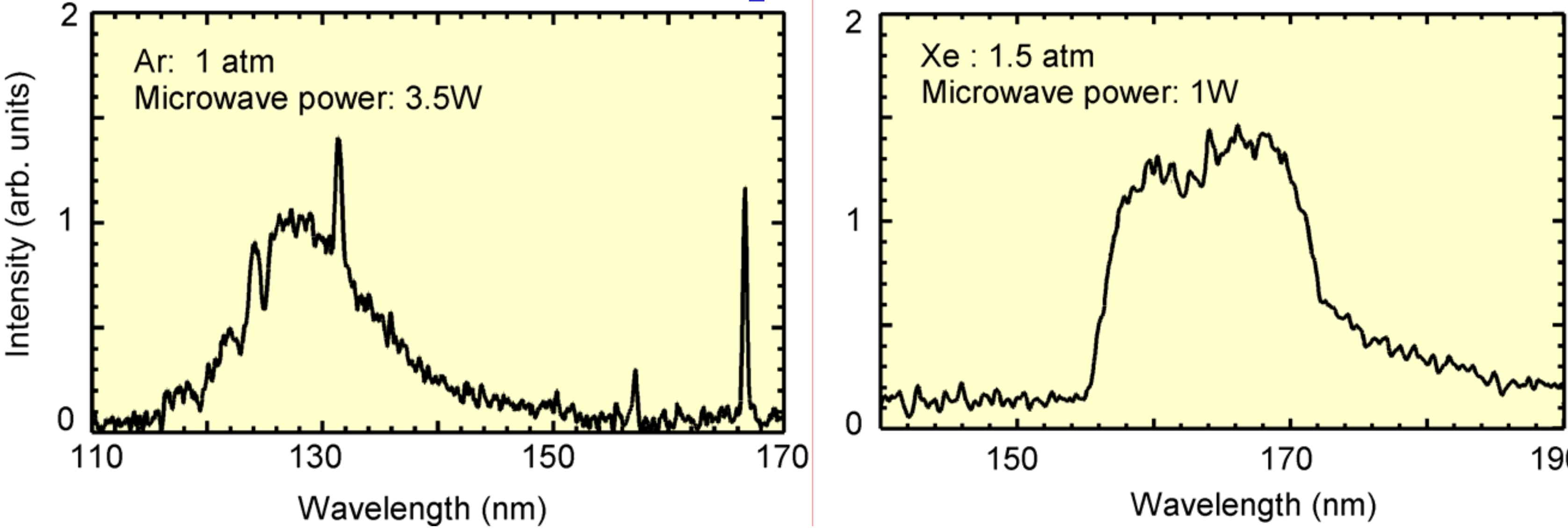

Power dependence (without gas flow)

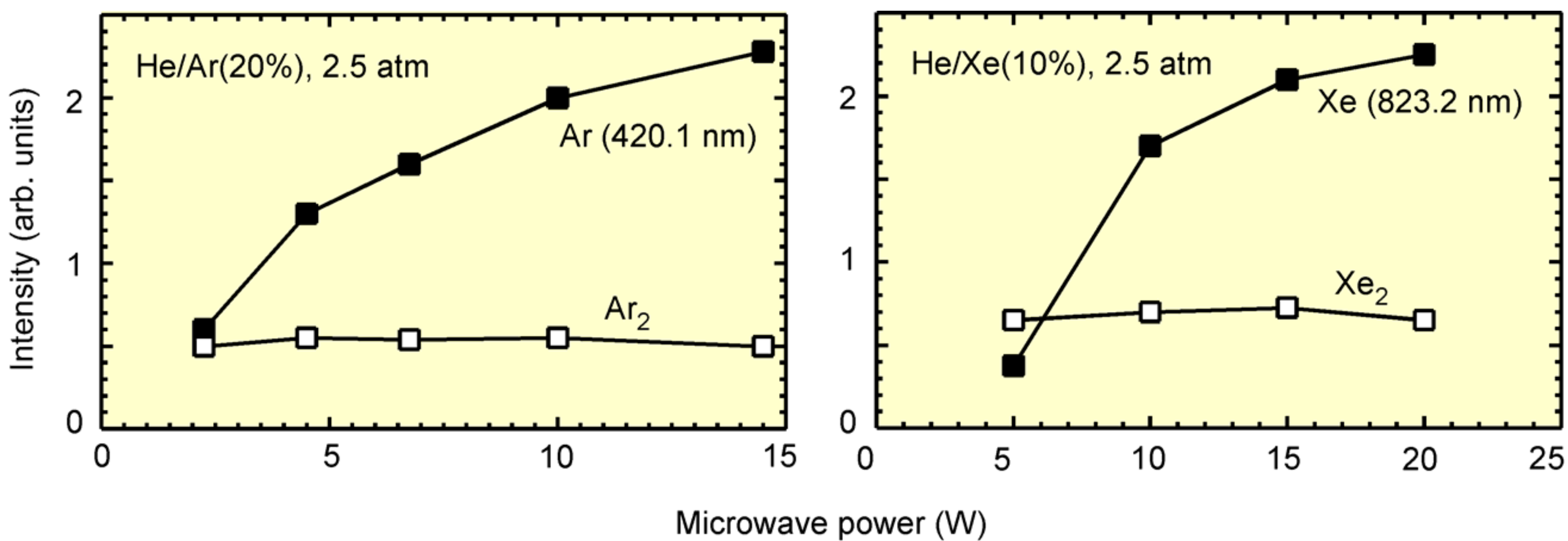

Gas Temperature study

* **OES measurements**
* **Fluid dynamic simulation of heat transport**

Power dependence of the gas temperature

(derived from N_2 $C^3\Pi_u$-$B^3\Pi_g$ optical emission)

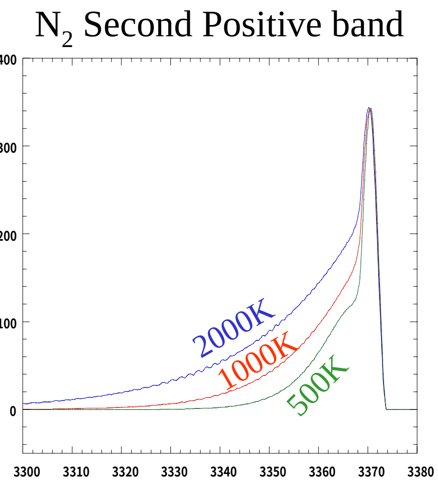

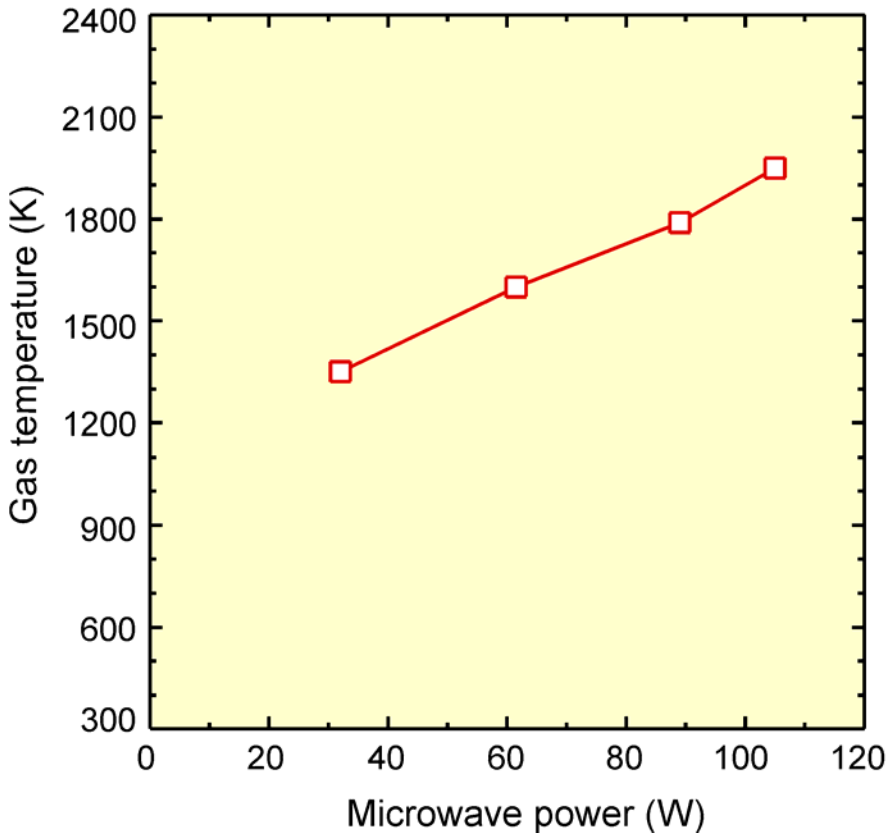

air 1atm ,
no gas flow

Weak dependence of T_g on $P_{\mu wave}$

Flow-rate dependence of the gas temperature

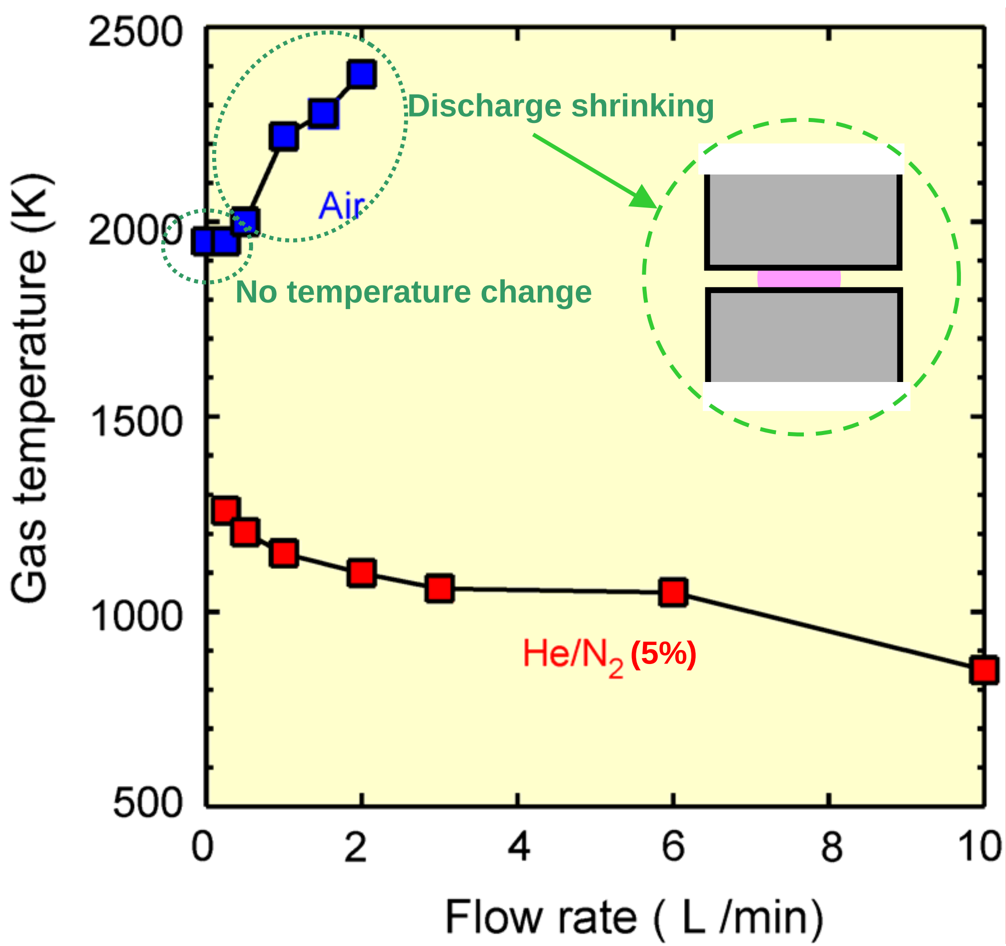

Open-air setup
1 atm
microwave power 100W

Temperature structure in the microgap discharge

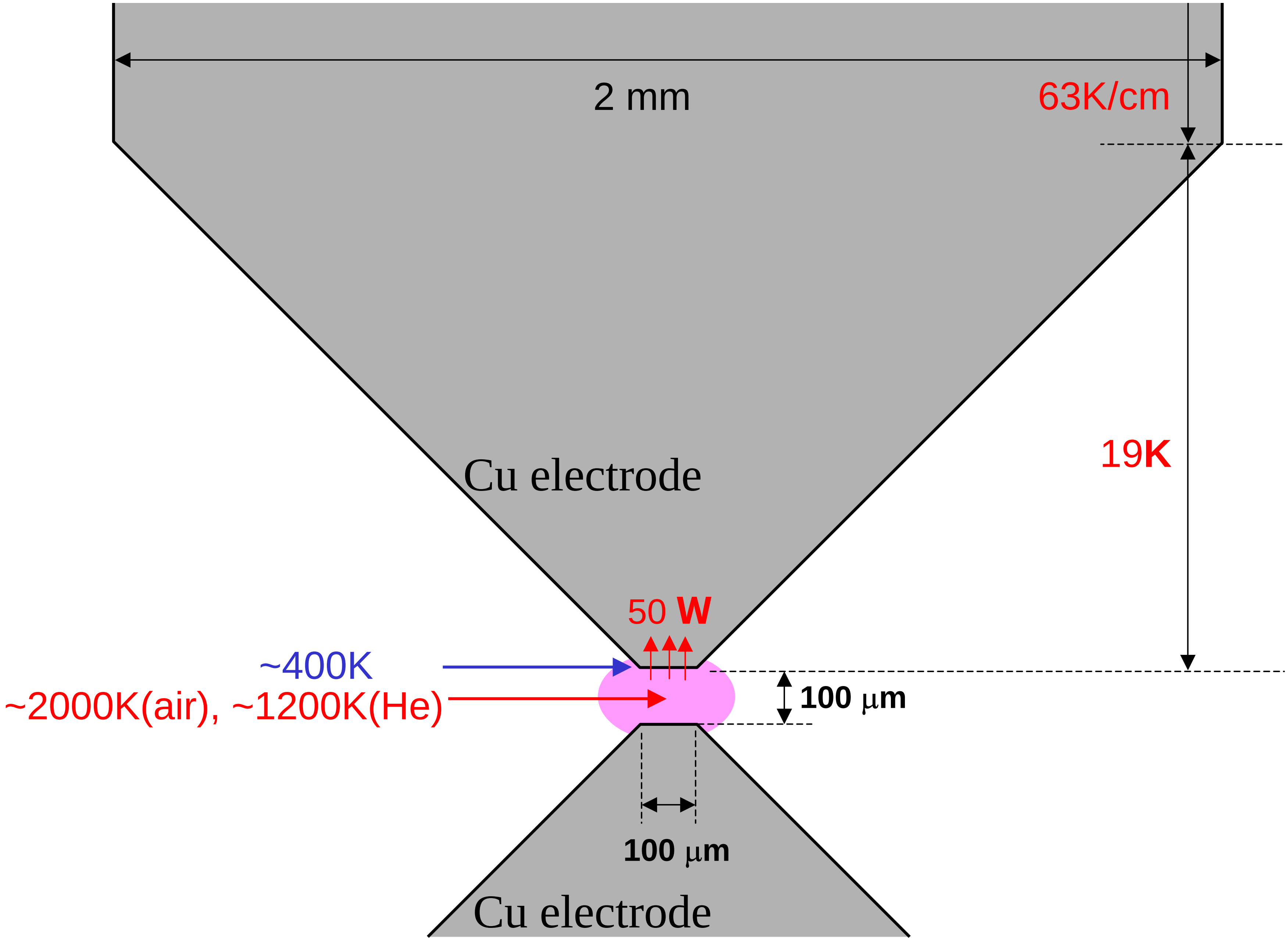

Heat transport simulation:
Simulation space and boundary conditions

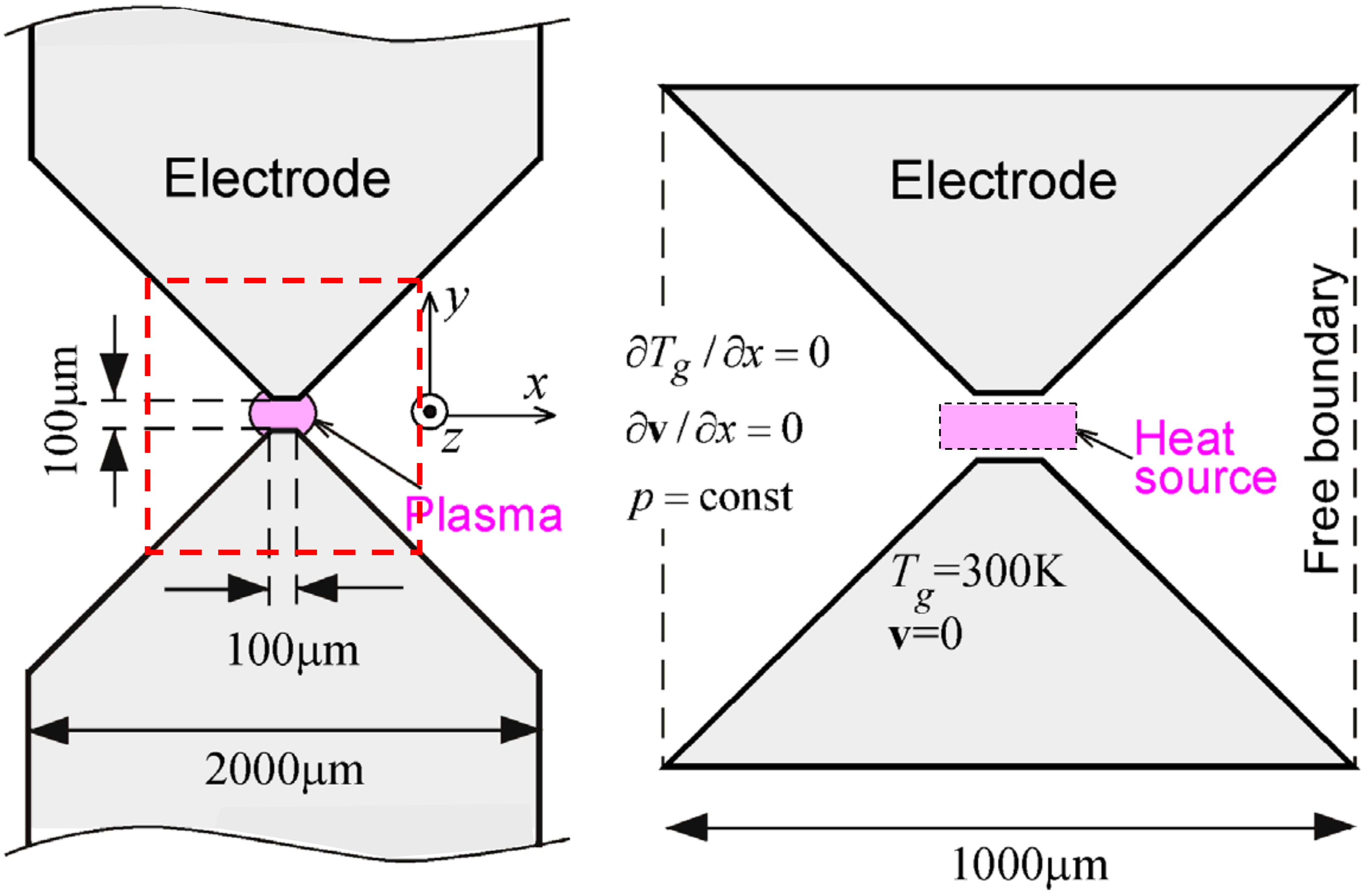

(a) Electrodes (b) Simulation space

Heat transport simulation: Governing equations

Mass balance

$$\frac{\partial \rho}{\partial t} + \nabla \cdot (\rho \ \mathbf{v}) = 0$$

Model (a): $Q = \text{const}$

Model (b): $Q = Q_0 \dfrac{\rho}{\rho_0}$

Momentum balance

$$\rho[\frac{\partial \mathbf{v}}{\partial t} + (\mathbf{v} \cdot \nabla)\mathbf{v}] = -\nabla p + \nabla \cdot \left\{ \eta(\nabla \mathbf{v} + [\nabla \mathbf{v}]^T) - \frac{2}{3}\eta(\nabla \cdot \mathbf{v})\mathbf{I} \right\}$$

Energy balance

$$\rho c(\frac{\partial T_g}{\partial t} + \mathbf{v} \cdot \nabla T_g) = \nabla \cdot (\kappa \ \nabla T_g) - p\nabla \cdot \mathbf{v} + (\nabla \mathbf{v}) : \left\{ \eta(\nabla \mathbf{v} + [\nabla \mathbf{v}]^T) - \frac{2}{3}\eta(\nabla \cdot \mathbf{v})\mathbf{I} \right\} + Q$$

Thermal conduction

Heating / cooling by adiabatic Compression / expansion

Heating by viscosity

Heat source (plasma)

$$\kappa = aT_g^{\ 0.77} \qquad \kappa = \frac{5}{2} \cdot \frac{c\eta}{m} \qquad p = \frac{\rho k T_g}{M}$$

Implication of n_e=10^{15} cm^{-3}

Gas heating by elastic collisions of electrons

$$Q = \frac{4}{\sqrt{\pi}}\left(\frac{2m}{M} T_e\right)(\sigma_m v_e) n_e n_g$$

$$\text{for} \begin{cases} n_e = 10^{15}\ \text{cm}^{-3} \\ n_g = 2.7\times 10^{19}\ \text{cm}^{-3}\ (1\ \text{atm}) \\ \sigma_m = 10^{-15}\ \text{cm}^2 \\ T_e = 2\ \text{eV} \\ m/M\ \text{for He} \end{cases} \Rightarrow Q = 0.45\ \text{MW/cm}^3$$

Gas temperature without gas flow

Profile

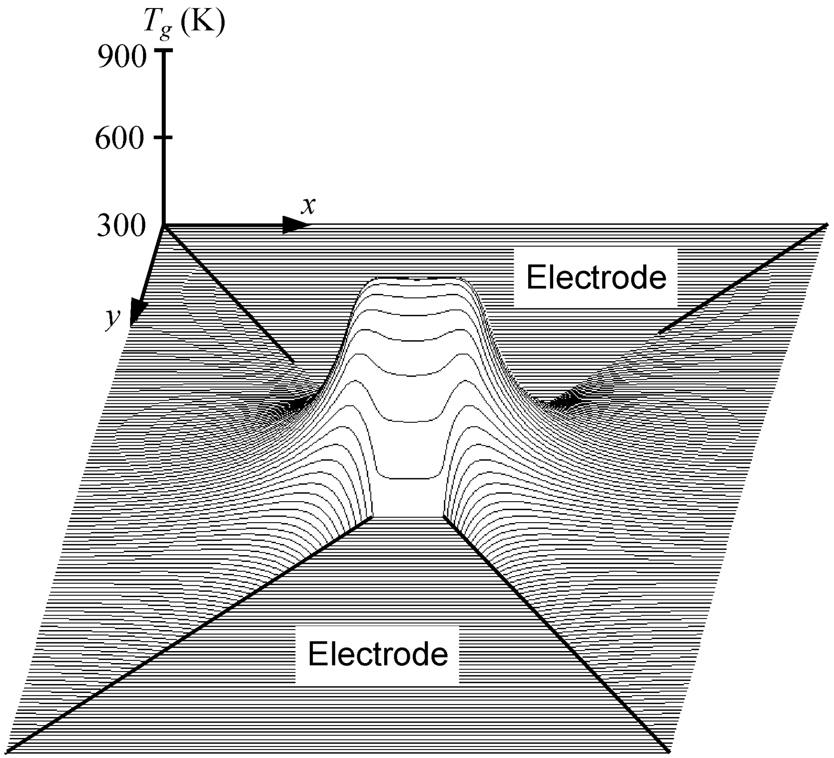

He, model (b), Q_0=0.5MW/cm^3

Dependence on Q or Q_0

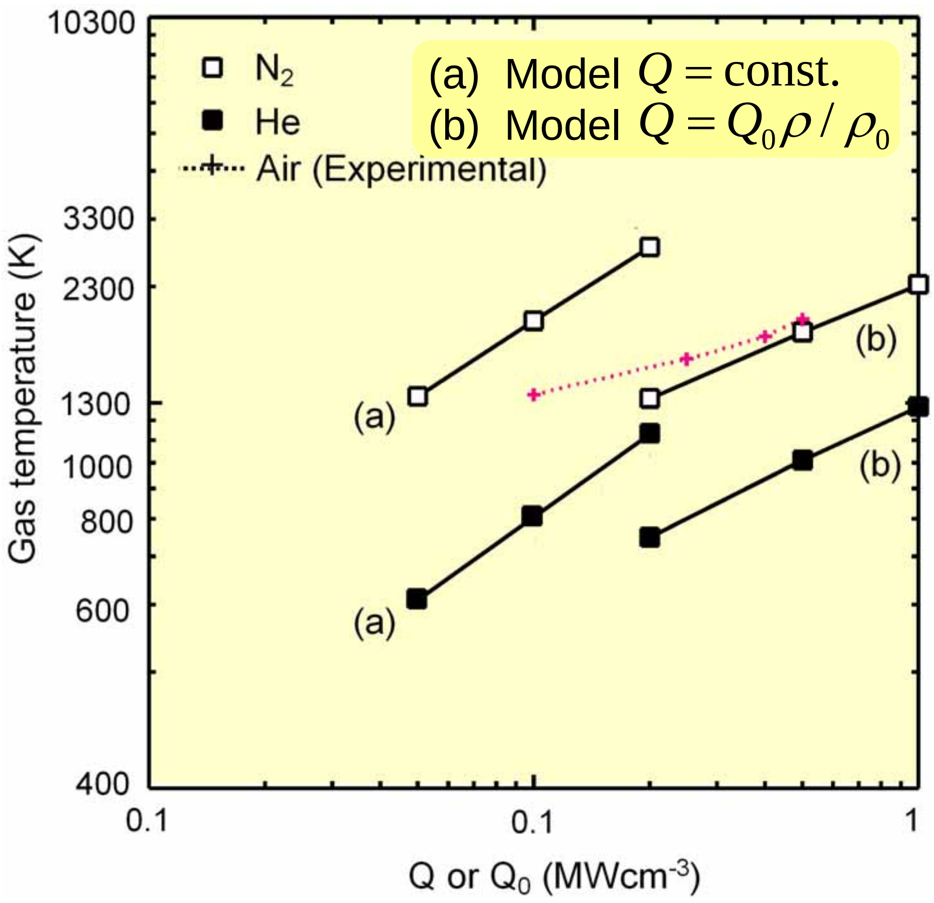

Effect of gas flow on the temperature profile

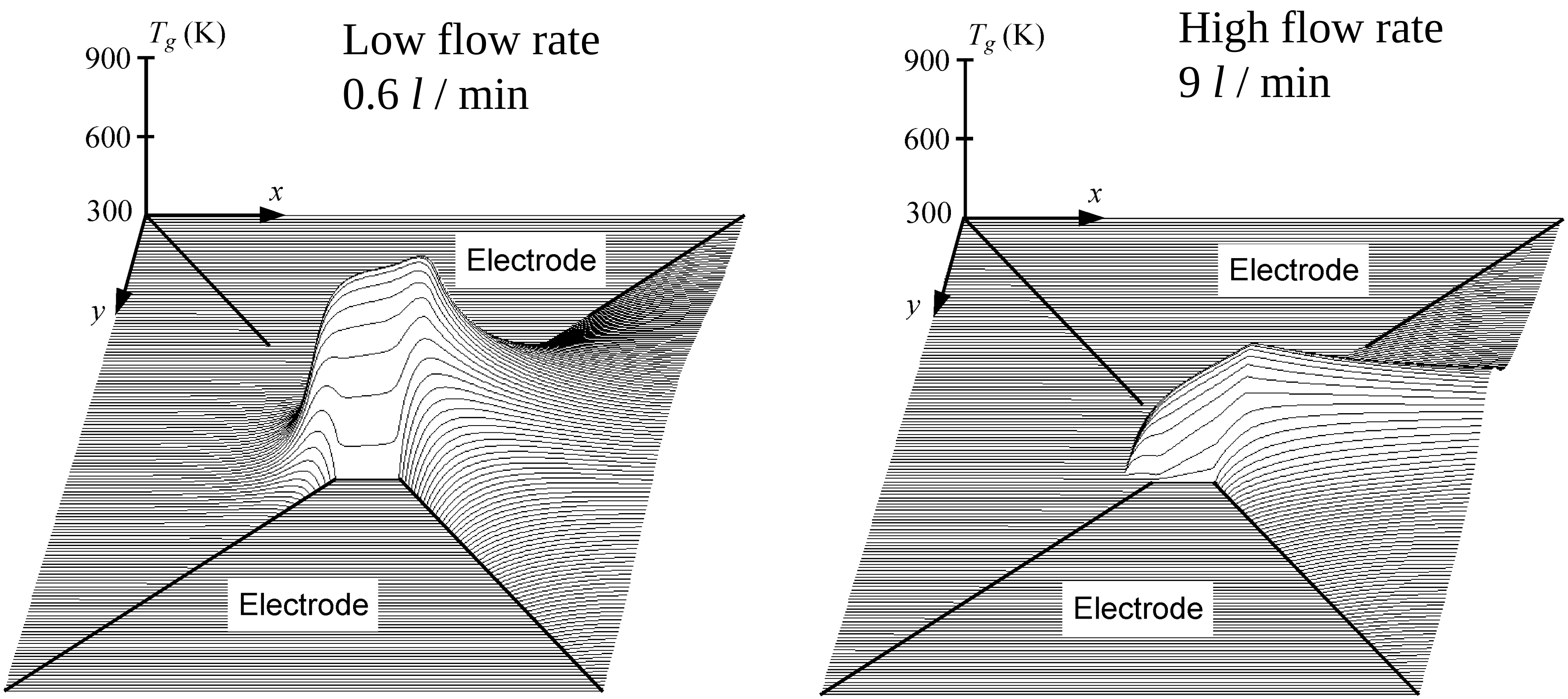

He, model (b), Q_0=0.5MW/cm^3

Dependence of the gas temperature on the gas flow

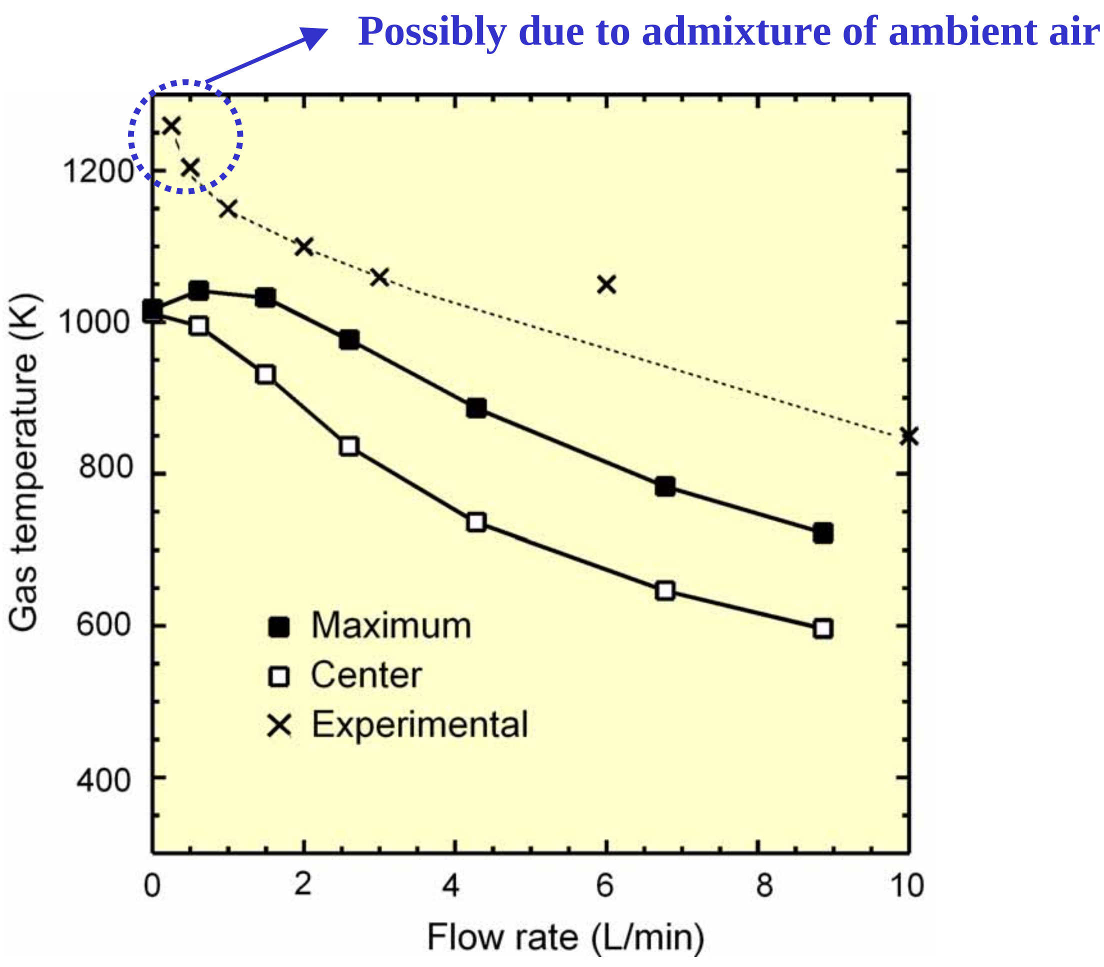

He, model (b), Q_0=0.5MW/cm^3

Gas heating and pressure loss

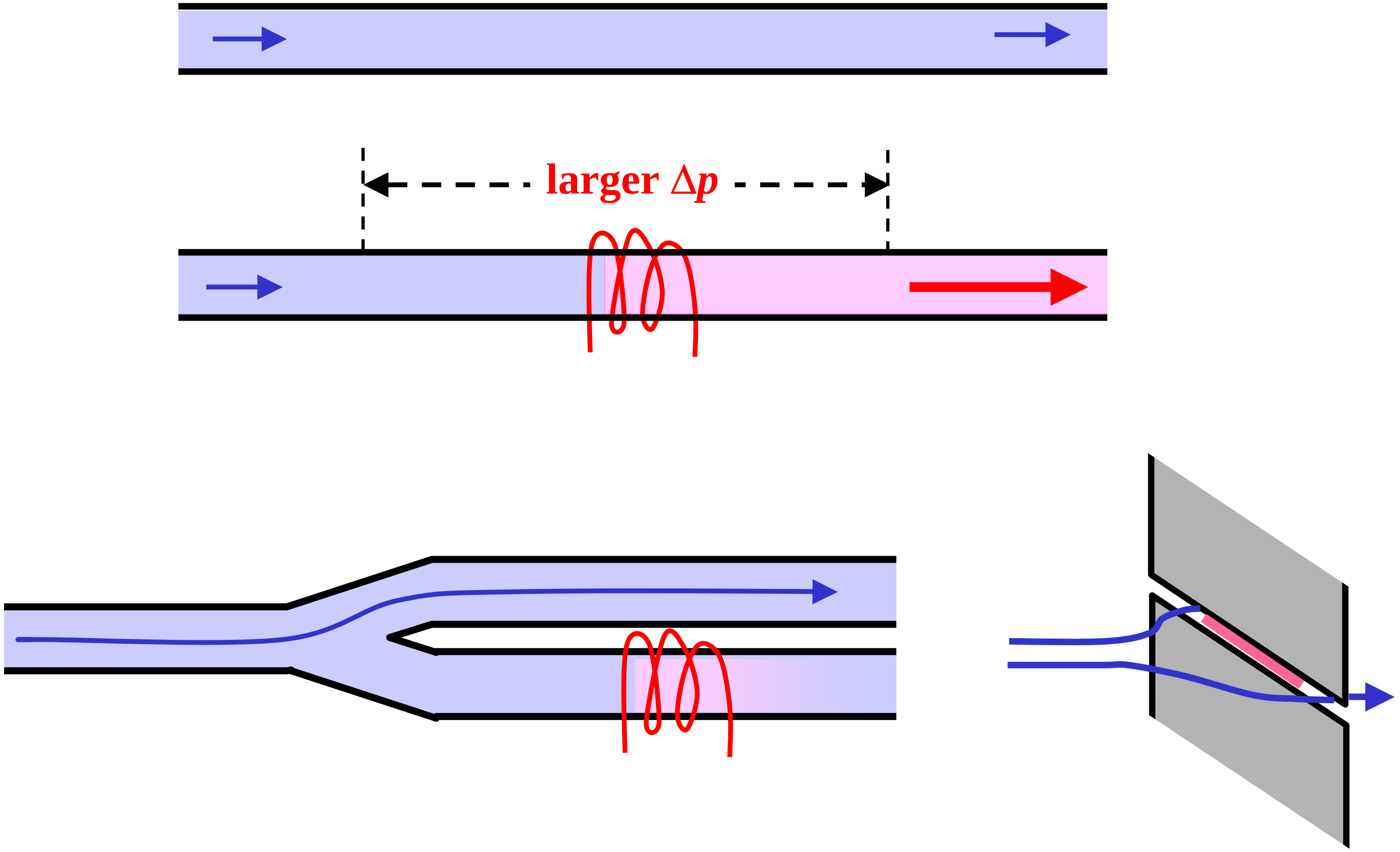

Unsuitable experimental setup

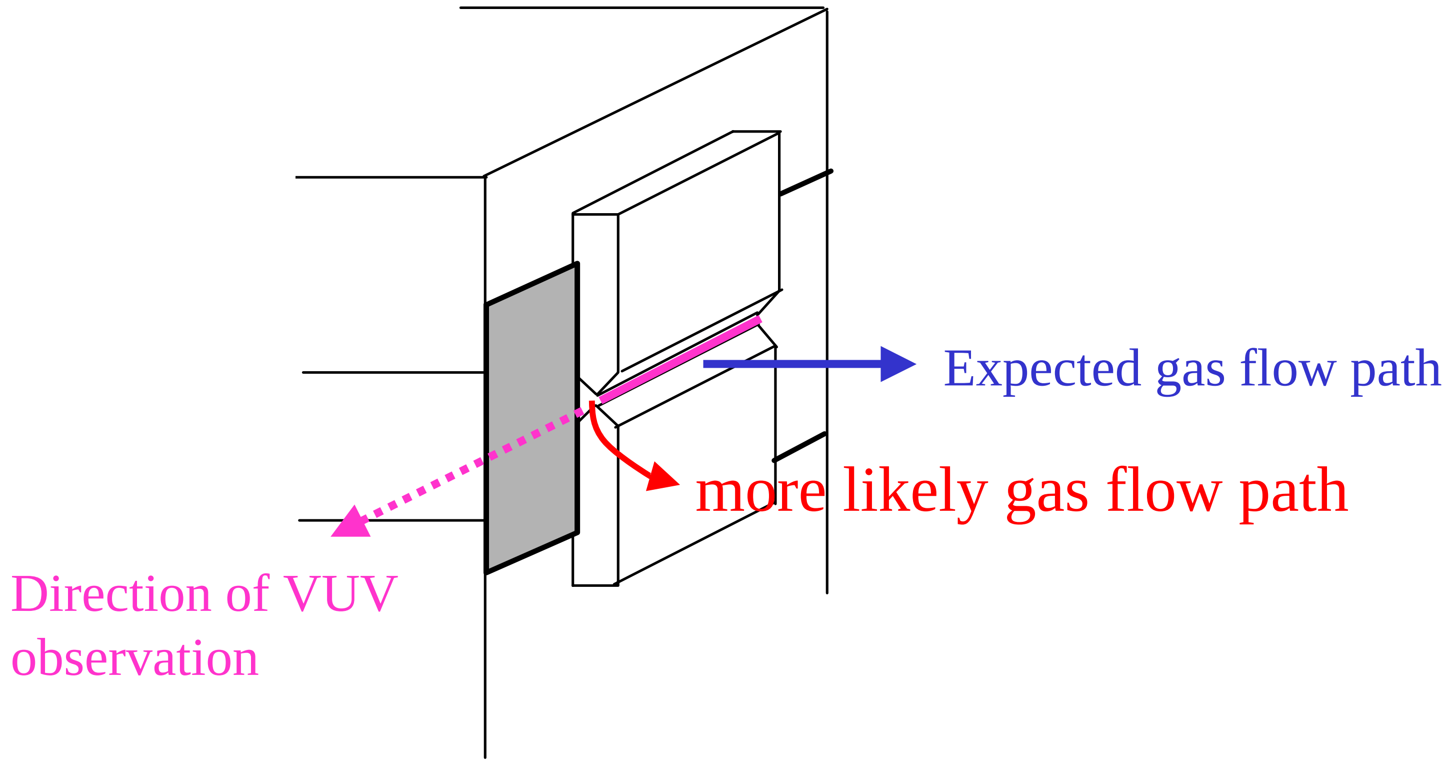

Ar_2 intensity vs. gas flow rate and pressure

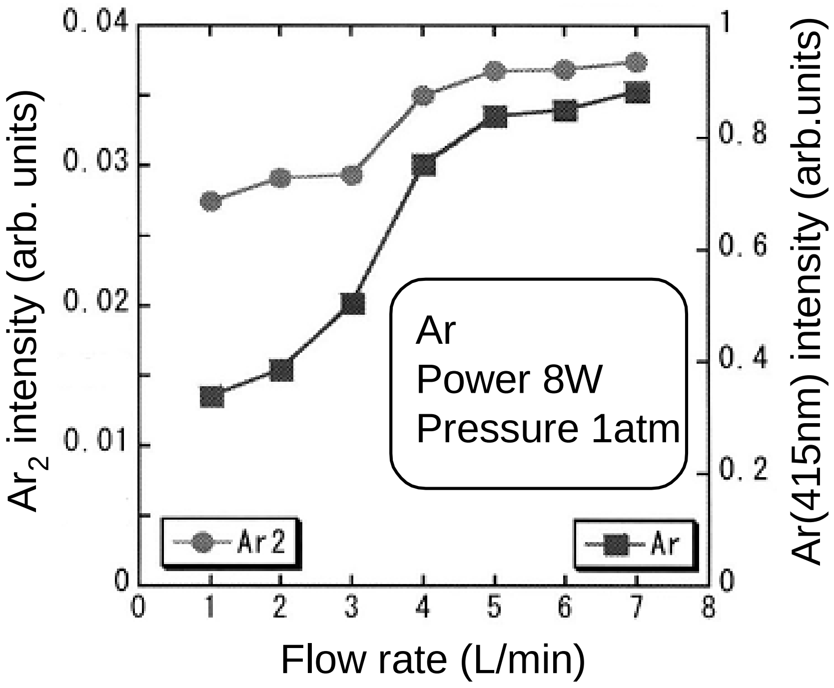

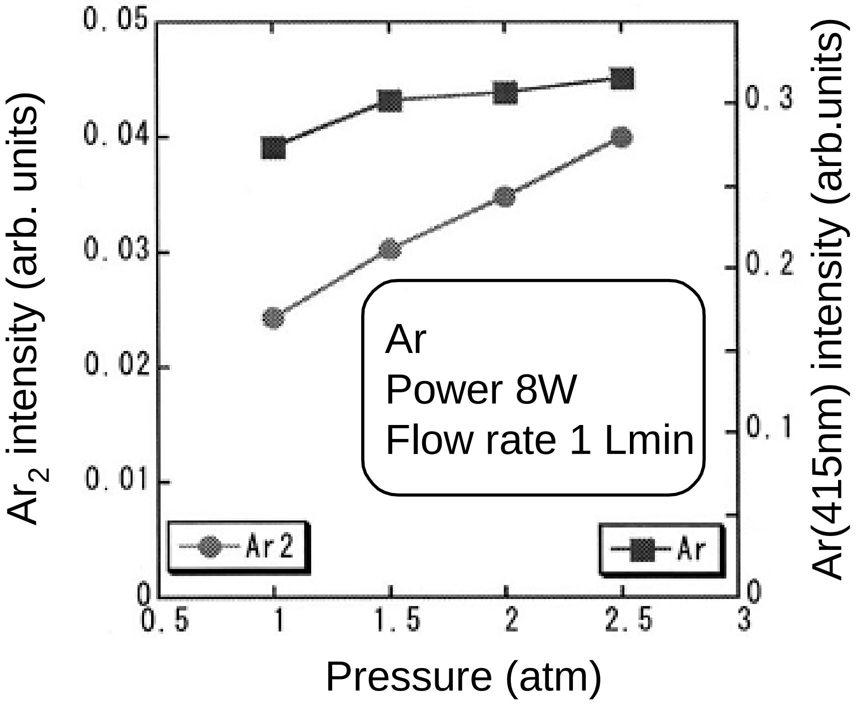

New gas flow scheme

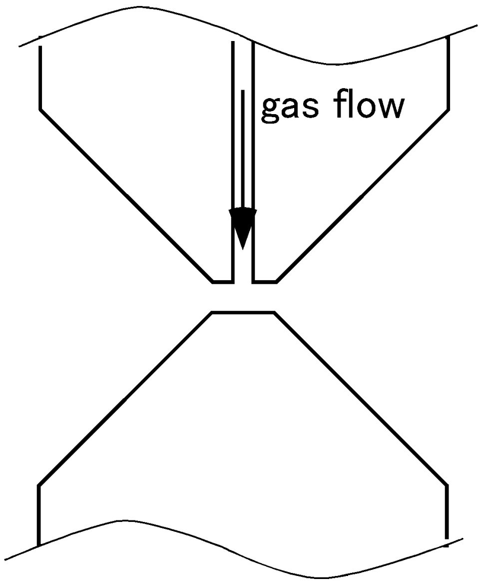

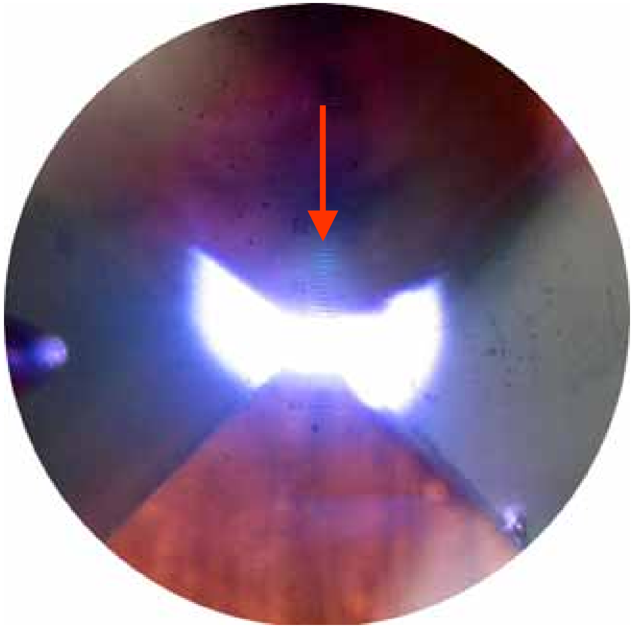

Summary

- Microwave excited microgap plasma
  - Stable *cw* production of high-pressure, high-density, non-thermal plasma over some length
  - Power deposition level of ~1 MW/cm^3
- High-spatial-resolution Thomson scattering measurement
  - Spatial resolution ~25 μm
  - n_e=1.8 x 10^{15} cm^{-3} for air discharge at 100 W
- Fluid dynamic simulation for heat transport
  - Importance of local gas density change for gas heating process
  - Need of selfconsistent treatment of plasma and gas dynamics
- To efficiently lower the gas temperature and to obtain efficient VUV excimer emission, the gas flow scheme is very important.

Future work： New gas flow scheme
Electron temperature control
Frequency upscaling